

Received 31 January 2016; revised 3 May 2016; accepted 11 May 2016. Date of publication 7 July, 2016; date of current version 23 August 2016.  
The review of this paper was arranged by Editor P. R. Berger.

Digital Object Identifier 10.1109/JEDS.2016.2571666

# Nanometer-Scale III-V MOSFETs

JESÚS A. DEL ALAMO<sup>1</sup> (Fellow, IEEE), DIMITRI A. ANTONIADIS<sup>1</sup> (Life Fellow, IEEE),  
JIANQIANG LIN<sup>1,2</sup> (Student Member, IEEE), WENJIE LU<sup>1</sup> (Student Member, IEEE),  
ALON VARDI<sup>1</sup>, AND XIN ZHAO<sup>1</sup> (Student Member, IEEE)

<sup>1</sup> Microsystems Technology Laboratories, Massachusetts Institute of Technology, Cambridge, MA 02139, USA

<sup>2</sup> Center for Nanoscale Materials, Argonne National Laboratory, Argonne, IL 60439, USA

CORRESPONDING AUTHOR: J. A. del ALAMO (e-mail: alamo@mit.edu)

This work was supported in part by the Korea Institute of Science and Technology, in part by the National Science Foundation under E3S STC Award 0939514, in part by the Defense Threat Reduction Agency under Grant HDTRA1-14-1-0057, in part by Northrop Grumman, in part by Samsung Electronics, in part by Applied Materials, and in part by Lam Research.

**ABSTRACT** After 50 years of Moore's Law, Si CMOS, the mainstream logic technology, is on a course of diminishing returns. The use of new semiconductor channel materials with improved transport properties over Si offer the potential for device scaling to nanometer dimensions and continued progress. Among new channel materials, III-V compound semiconductors are particularly promising. InGaAs is currently the most attractive candidate for future III-V based n-type MOSFETs while InGaSb is of great interest for p-channel MOSFETs. At the point of most likely deployment, devices based on these semiconductors will have a highly three-dimensional architecture. This paper reviews recent progress toward the development of nanoscale III-V MOSFETs based on InGaAs and InGaSb with emphasis on scalable technologies and device architectures and relevant physics. Progress in recent times has been brisk but much work remains to be done before III-V CMOS can become a reality.

**INDEX TERMS** III-V compound semiconductors, CMOS, InGaAs, InGaSb.

## I. INTRODUCTION

Si CMOS has been the engine that has powered the microelectronics revolution for the major part of the last 50 years. MOSFET scaling and its "triple dividends" of cost reduction, enhanced performance and greater energy efficiency, has made this possible. This extraordinary feat of human innovation is facing unprecedented challenges. Several features of MOSFETs long held at the heart of its unique suitability for logic circuits had to be replaced in the last few years: the SiO<sub>2</sub> gate oxide has given way to "high-K" (high permittivity) dielectrics and the planar structure has been superseded by FinFETs. Perhaps the time has come to discard Si itself as the active channel material.

One of the central difficulties of Si MOSFETs is the increase in parasitic capacitance and resistance relative to their intrinsic counterparts as device dimensions decrease. At a time when voltage reduction is imperative in order to manage power dissipation, increased parasitics translate into performance, i.e., current drive, that has stagnated. A potential solution to this is to substitute the Si channel by a new material where carriers travel at higher velocity. All things

being equal, this should yield higher current and improved performance.

It is in this regard that certain III-V compound semiconductors have a lot to offer [1]. InGaAs for electrons and InGaSb for holes offer a good balance among the many requirements imposed on a MOSFET channel material: high mobility, low contact resistance, sufficient interfacial quality with high-K dielectrics and adequate bandgap energy. In addition, the InGaAs heterostructure system is relatively mature with InGaAs High Electron Mobility Transistors (HEMT) and Heterojunction Bipolar Transistors (HBT) at the heart of many advanced communication systems as well as in low-cost mass-market applications such as cellular phones [2].

The last few years have witnessed an explosion of research on InGaAs-based n-channel MOSFETs in industry and academia. This has delivered rapid progress in planar device designs as well as 3D architectures such as FinFETs and nanowire FETs [3]–[5]. For alternative p-type MOSFETs, Ge channels look very promising but InGaSb has also advantageous properties that make it attractive [1]. Much less research has been devoted to this latter topic but

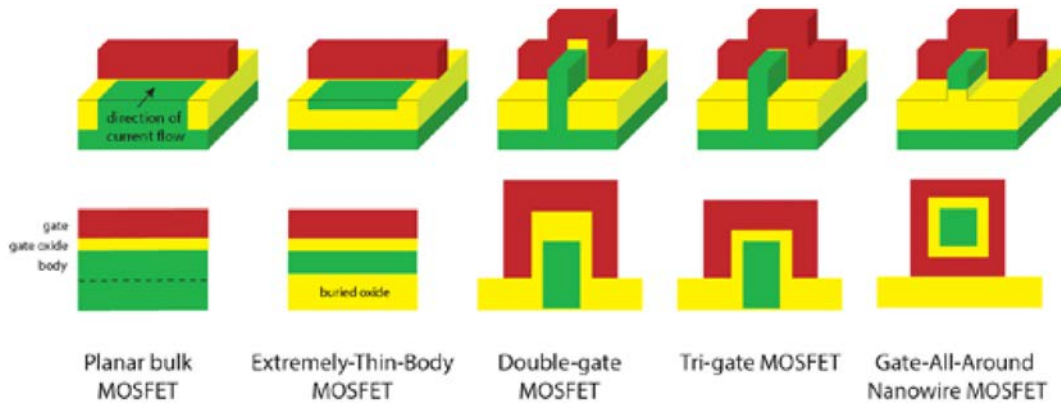


**FIGURE 1.** 3D schematic (top) and cross-sectional schematic (bottom) of MOSFET structures with increasing electrostatic gate control of the channel from left to right. In Planar bulk and Extremely-Thin-Body MOSFETs, channel charge is electrostatically controlled by gating from the device surface. In Double-gate MOSFETs, gate action takes places from two side surfaces of a fin-shaped channel. In Tri-gate MOSFETs, the gate wraps around three sides. The “Gate-All-Around” nanowire MOSFET, in its horizontal or vertical configuration, has a thin nanowire channel that is wrapped around its entire periphery by the gate.

recent results suggest InGaSb is a candidate worthy of close examination [6], [7].

This paper reviews recent progress towards the development of III-V n-channel and p-channel MOSFETs for future CMOS applications. The paper emphasizes recent developments on Si-compatible technologies and scalable transistor architectures as well as novel device physics of relevance to future logic CMOS. The paper is organized as follows. Section II deals with thin-body InGaAs planar device architectures. Section III concerns InGaAs FinFETs and Trigate FETs. Section IV reviews progress on InGaAs Nanowire MOSFETs. Finally, Section V summarizes recent research on InGaSb MOSFETs. For lack of space, the very important issues of III-V materials integration with Si wafer manufacturing is not discussed in this paper.

## II. INGAAS PLANAR MOSFETS

Fig. 1 shows the evolution of MOSFET architecture in its quest for reduced footprint, enhanced transistor density and lower cost, the drivers of Moore’s law. The challenge in transistor scaling is maximizing performance (i.e., drain current density) at reduced voltage while keeping short-channel effects in check. Footprint scaling demands shrinking all dimensions, including the gate length, in a harmonious way. Mitigating short-channel effects as gate length scales down, requires enhanced gate control of the channel. This has dictated looking beyond the planar bulk or thick SOI MOSFET to ultra-thin body MOSFET and eventually to so-called multi-gate structures such as the Double-Gate MOSFET, Trigate MOSFET (both referred to here as FinFETs) and the Gate-All-Around Nanowire MOSFET in a horizontal or vertical configuration. All these device structures have been demonstrated in the InGaAs system [3].

As the simplest possible structure, the planar InGaAs MOSFET has made great strides in recent times. The Quantum-Well (QW) MOSFET configuration, with a very thin quantum confined channel, has delivered the best results

as it provides excellent electrostatic control from the top gate. As a measure of the progress that has recently been achieved, Fig. 2 shows the evolution of transconductance,  $g_m$ , of InGaAs MOSFETs (undoped body) and HEMTs as a function of year of demonstration.  $g_m$  is a critical figure of merit in just about any transistor application. While the first InGaAs MOSFETs were reported at about the same time as the first HEMTs appeared on the scene over 30 years ago, there has been a striking transconductance gap between the two types of devices that lasted for over 25 years. It is only recently that the InGaAs MOSFET has emerged as a viable transistor architecture. In fact, only this year the  $g_m$  of an InGaAs MOSFET has come to exceed that of the best InGaAs HEMT [8].

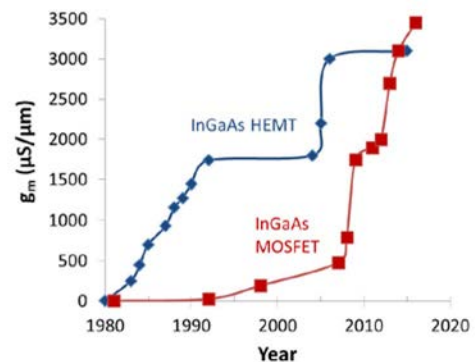


**FIGURE 2.** Transconductance comparison of InGaAs MOSFETs (undoped body) and HEMTs (with InAs composition between 0 and 1) vs. year of demonstration.

The dramatic emergence of InGaAs MOSFETs in the last few years would not have been possible without solving a long-standing problem in III-V MOS systems and that is Fermi level pinning at the oxide-semiconductor interface. Fermi level pinning is believed to be due to the formation of native oxides that create high concentration of defects at the semiconductor surface [9]. Fermi

level pinning prevents the modulation of the surface potential by the gate and the charge control that is essential for the operation of a MOSFET. A technological breakthrough has recently addressed this problem. This was the finding that the use of atomic layer deposition (ALD) to form the gate oxide involves a “self-cleaning effect” that eliminates the native oxides and associated defects at the semiconductor surface [10], [11]. Fast forward a few years and after several fundamental studies [12]–[14] and there are now many demonstrations of high-permittivity oxide/InGaAs interfaces with very high quality. Subthreshold swings in MOSFETs with values approaching 60 mV/dec have been demonstrated [15]–[17]. Interface state densities in the  $10^{11}$  eV<sup>-1</sup>.cm<sup>-2</sup> range have also been reported [18], [19].

Another key element that has greatly contributed to the dramatic recent improvement in InGaAs MOSFET performance has been the development of self-aligned device architectures. Self-alignment of gate and contacts is essential for manufacturability and to minimize parasitics and footprint. In essence, four different self-aligned designs have emerged in the last few years. A contact-first, gate last process in which the gate is nested in an opening created in the ohmic contacts has yielded excellent results [8], [16], [20]–[22]. The extensive use of Reactive Ion Etching (RIE) has afforded very tight contact-gate spacing and high performance. A schematic diagram of this device is shown in Fig. 3.

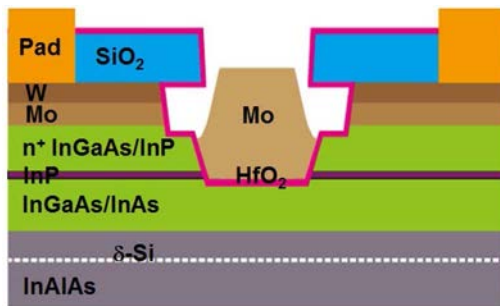


**FIGURE 3.** Cross-sectional schematic of a self-aligned InGaAs Quantum-Well MOSFET fabricated by a contact-first, gate-last process [21].

An alternative approach that has also delivered good results consists of raised, self-aligned source and drain epitaxial regions selectively grown around a gate or a dummy gate [23]–[25]. By virtue of the high doping that can be introduced in the source and drain contact regions, this design has yielded very small parasitic access resistance [24].

In yet another approach, a thin Ni layer is thermally reacted with InGaAs to give rise to a highly conducting and very shallow intermetallic compound with very low resistivity [26], [27]. The unreacted Ni can be selectively removed. This is exploited to fabricate self-aligned InGaAs MOSFETs in a process akin to that of silicided

source and drain Si MOSFETs [28], [29]. The performance of such devices is lagging because of the relatively large contact resistance of the NiInGaAs/InGaAs system.

In a final approach, the combination of self-aligned ion implanted source and drain extensions and in-situ doped raised source and drain regions around a gate has also been used to fabricate self-aligned InGaAs MOSFETs with excellent characteristics [30].

In nanometer-scale transistors in which the space available for the ohmic contacts is very limited, achieving very low contact resistance is a critical issue. Fig. 4 compares different Si-compatible ohmic contact schemes to  $n^+$ -InGaAs in terms of the most important performance metrics: contact resistivity and metal film resistivity [31]. Both need to be small in order to minimize the contact resistance in actual transistor structures. The lowest contact resistivity has been obtained in the Pd-InGaAs system [32], however, its film resistivity is poor. On the other hand, refractory metals such as Mo and W have yielded excellent contact resistivity and also feature very low film resistivity [33]. Even with these materials, at the dimensions of interest, the best contact resistance that has been demonstrated is still too high by at least a factor of two [31]. A contact resistivity below  $0.1 \Omega \cdot \mu\text{m}^2$  is required to accomplish the desired objective. This is a very challenging goal.

The path forward will require superior understanding and control of the metal-semiconductor interface. There is clear evidence that a contact-first approach protects the integrity of the interface and yields outstanding contacts [33], [34]. This highlights the promise of careful engineering of the metal/semiconductor interface. The Landauer limit for contacts to  $n^+$ -In<sub>0.53</sub>Ga<sub>0.47</sub>As for practical doping levels is in the  $0.1 \Omega \cdot \mu\text{m}^2$  range [35]. Higher doping levels should enable to reach below this value. In addition, the Schottky barrier height of metals on InGaAs can be engineered over a relatively wide range of values through the InAs composition at the surface [28].

Planar MOSFETs are limited in their scaling potential. This has become evident in a recent channel scaling study in which the gate length and channel thickness of self-aligned QW-MOSFETs was varied over a broad dimensional range [21]. Channel thickness was found to have a strong impact on device characteristics. A thick channel is beneficial to ON-state figures of merit, such as  $g_m$ , while a thin channel benefits OFF-state metrics, such as subthreshold swing,  $S$ , and drain-induced barrier lowering (DIBL). In fact,  $S$  and DIBL were found to follow classic scaling behavior. These observations are borne by other results in the literature. Fig. 5 shows linear  $S$  (low  $V_{ds}$ ) vs. the ratio of the gate length to the electrostatic length for published InGaAs QW-MOSFETs. Many device demonstrations have been made that approach ideal electrostatic scaling behavior. The conclusion from this is that InGaAs QW MOSFETs are at the limit of scaling around  $L_g = 50$  nm beyond which short-channel effects become too severe.

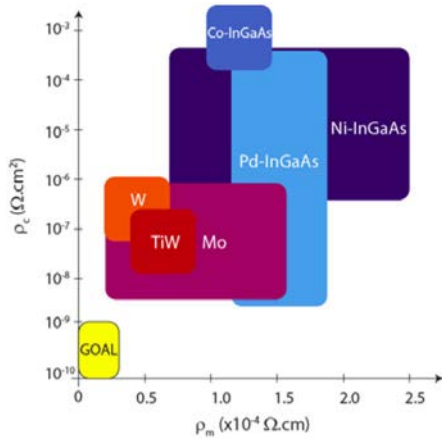


**FIGURE 4.** Landscape of contact resistivity vs. metal film resistivity of Si-compatible ohmic contacts to n-InGaAs [31]. The desired regime of operation is the bottom left corner.

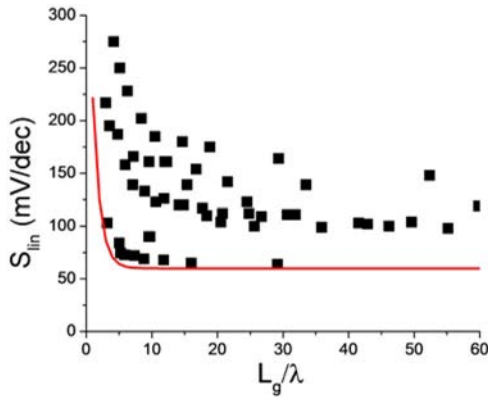


**FIGURE 5.** Linear subthreshold swing vs. ratio of gate length to electrostatic scaling length of planar InGaAs Quantum-Well MOSFETs from the literature. The line indicates the expected theoretical behavior based on a simple model [21].

Planar MOSFETs, though unable to meet the scaling goals, constitute an excellent platform for process development and device physics exploration. A recent example is the identification of the physics behind the excess off-state current that has been observed in tight-pitch InGaAs QW-MOSFETs and that prevents transistors from being effectively shut off [36], [37]. As Fig. 6 shows, the excess off-state current is strongly enhanced by  $V_{ds}$  and it also increases as the gate length scales down which makes this phenomenon highly problematic in nanoscale devices.

A detailed experimental and modeling study has revealed that the excess off-state current is due to band-to-band tunneling (BTBT) at the drain-end of the channel that is amplified by the parasitic lateral bipolar transistor formed by the channel (floating base), the source (emitter) and drain (collector) of the MOSFET [37]. With a base made out of InGaAs, the lateral bipolar transistor current gain can be very high, order  $\sim 10^3$ , so that even a small BTBT-generated current can result in sizable off-state leakage current. This deleterious phenomenon is a consequence of

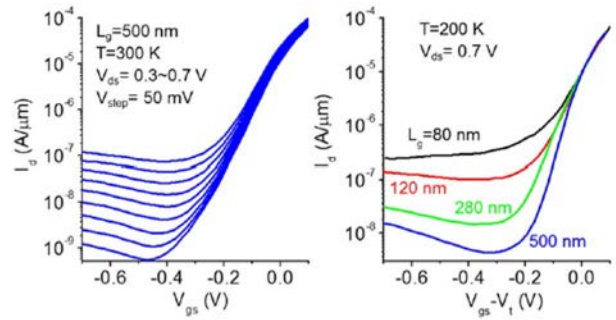


**FIGURE 6.** Subthreshold characteristics of self-aligned InGaAs MOSFETs showing weak  $V_{gs}$  control of off-state current. Left: long-channel device as a function of  $V_{ds}$  at room temperature. Right: devices with different gate lengths at  $V_{ds} = 0.7$  V and at 200 K [36], [37].

the small bandgap of the InGaAs channel and from the fact that BTBT-generated holes cannot be easily extracted from the channel. As a consequence, this problem will affect all InGaAs transistor architectures unless a hole contact can be provided to the body of the transistor. Mitigating this problem is a key goal for future scaled devices.

### III. INGAAS FINFETS

Improved MOSFET scalability over what planar devices can deliver requires 3D, or multigate, device designs. Double-gate or triple-gate (Trigate) InGaAs FinFETs (see Fig. 1) provide enhanced gate control over the channel yielding greater scaling potential. In commercial Si CMOS technology, FinFETs currently constitute the structure of choice for leading edge devices [38], [39].

InGaAs double-gate and Trigate FinFETs have been demonstrated by several groups [15], [40]–[45]. Top-down approaches based on RIE are common [15], [40], [41], [43]–[45], while bottom-up approaches using Aspect Ratio Trapping (ART) [46] have also been explored [42]. At the moment, InGaAs transistors fabricated by either of these techniques have demonstrated modest performance when compared with what is to be expected.

A summary of the state of the art for InGaAs FinFETs concerning carrier transport characteristics, can be seen in Fig. 7. This graph shows the peak transconductance demonstrated in InGaAs FinFETs to date as a function of fin width,  $W_f$ . For reference, estimations from selected state-of-the-art Si FinFETs have been included [38], [39]. In this figure,  $g_m$  has been normalized by the total conducting gate periphery (number of fins  $\times (2H_c + W_f)$ , where  $H_c$  is the channel height), as commonly done in FinFETs. The label next to each data point is the aspect ratio of the conducting channel in the fin ( $H_c/W_f$ ). The figure highlights recent results from some of the present authors (red squares) [45].

Several observations can be made from Fig. 7. First, published InGaAs FinFETs prior to those in [45] are based on relatively wide fins with channel aspect ratios that are, at best, unity. With the exception of [45], no transistors have

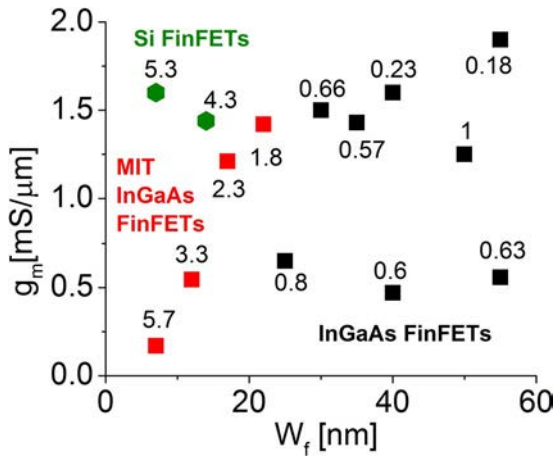


**FIGURE 7.** Benchmark of transconductance normalized by conducting gate periphery for InGaAs and Si FinFETs (estimated) as a function of fin width. The number next to each symbol gives the aspect ratio of the channel. Recent results from some of the present authors are highlighted with red symbols [45].

been reported with  $W_f < 25$  nm or channel aspect ratios greater than 1. This is in contrast with Si FinFETs where  $W_f < 10$  nm and channel aspect ratio in excess of 5 constitute the state of the art [39]. For future InGaAs FinFETs to realize the potential of this material system, far more aggressive fin designs are required [47].

The second observation to be made from the data of Fig. 7, though more subtle, is that InGaAs FinFETs are rather subpar when compared with Si FinFETs. The Si devices manage to extract a lot of  $g_m$  out of a tiny fin footprint, suggesting effective charge control from the sidewalls. In contrast, the InGaAs FinFETs have very large footprint and relatively short sidewalls and, nevertheless, they barely match the  $g_m$  of Si FinFETs. In fact, the InGaAs FinFETs in Fig. 7 are significantly worse than planar InGaAs MOSFETs where a peak  $g_m$  well in excess of 3 mS/ $\mu$ m has been demonstrated [8]. This is even though the experimental InGaAs FinFETs prototyped to date feature a relatively large contact area supplying current to comparatively narrow fins.

There are many reasons for this significant performance gap. In InGaAs FinFETs with etched fins, the majority of the data in Fig. 7, the quality of the sidewalls is a major concern. Sidewall roughness, relatively high interface state density on the sidewall MOS [48] and probably damaged sidewall stoichiometry [49] are undesirable byproducts of the etch process. In addition, in spite of the comparatively large contact area, access resistance in FinFETs tends to be significantly higher than in planar designs. This need not be the case, since Mo contacts on InGaAs fins have been demonstrated with contact resistance comparable to that of equivalent planar structures [50].

A key advantage of FinFETs is its enhanced scalability. As argued in the introduction, this stems from greater channel charge control. InGaAs FinFETs to date have indeed demonstrated excellent short-channel effects, as illustrated

in Fig. 8. This figure shows linear subthreshold swing in experimental devices that approach the expected ideal scaling behavior [51]. It is this that makes the FinFET architecture a very promising one for deeply scaled devices.

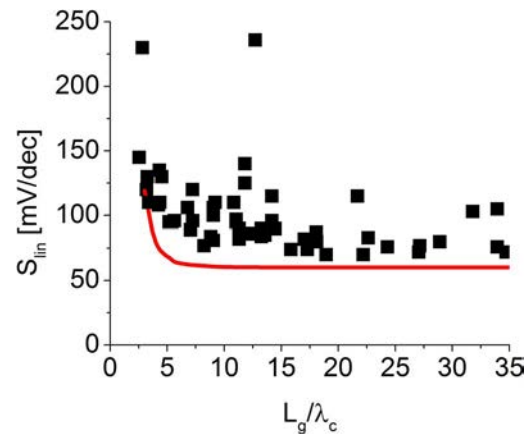


**FIGURE 8.** Linear subthreshold swing (low  $V_{DS}$ ) vs. ratio of gate length to electrostatic scaling length in experimental InGaAs FinFETs. For reference, the red line indicates ideal electrostatic behavior [51].

An issue of concern in scaled InGaAs FinFETs is the strong dependence of electrical parameters on the fin width as a consequence of quantum confinement effects. This is expected to be much worse than in equivalent Si FinFETs due to the low effective mass of electrons in InGaAs [52]. Recent experiments have verified these predictions in doped-channel InGaAs FinFETs that were fabricated by a precision dry etching process [53]. For fins narrower than about 10 nm, a strong fin width dependence to the threshold voltage,  $V_T$ , was observed as shown in Fig. 9. The width sensitivity of  $V_T$  is about four times larger than in Si FinFETs with equivalent fin widths. Fig. 9 also shows a comparison of experimental with simulated  $V_T$  from Poisson-Schrodinger simulations of InGaAs FinFETs [53]. The agreement between model and simulations strongly supports the quantum origin of this phenomenon. This has important implications for the design and manufacturing of future InGaAs FinFETs.

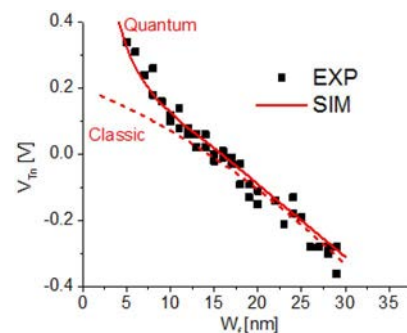


**FIGURE 9.** Experimental vs. simulated threshold voltage of n-InGaAs FinFETs (double gate) vs. fin width. The quantum model gives the result of self-consistent Poisson-Schrodinger simulations (Nextnano). The classic model does not include quantum effects [53].

#### IV. INGAAS NANOWIRE MOSFETS

The ultimate scalable MOSFET design is the nanowire architecture (Fig. 1). Nanowire MOSFETs come in two different geometries, horizontal and vertical. Both have been demonstrated in the InGaAs system.

*Horizontal* nanowire MOSFETs are essentially FinFETs in which the channel has been suspended through selective etching and a gate is wrapped around its entire periphery [19], [54]. This provides enhanced charge control and an ability to scale to smaller dimensions. Lateral InGaAs nanowires are more frequently prepared through etching, though lateral growth of GaAs and InAs nanowires has been demonstrated by the Vapor-Liquid-Solid technique [4]. Reviews of the state of the art in III-V Nanowire MOSFETs have recently been published [3], [4].

The *vertical* nanowire (VNW) MOSFET is a particularly attractive design because with a vertical current flow, footprint scaling and gate length scaling become uncoupled. This promises high transistor density, stemming from a very small footprint, yet acceptable short-channel effects due to the flexibility in  $L_g$  design [55]. In addition, there is also greater freedom in the selection of contact length as well as the length of the gate to ohmic contact spacer since neither contribute to the footprint. This should translate into lower contact resistance and parasitic capacitance and higher performance.

An intriguing aspect of VNW-MOSFETs is that they offer a plausible path for integration on a Si substrate. Bottom-up growth of InGaAs nanowires on Si substrates is relatively well established through Vapor-Liquid-Solid (VLS) epitaxy and selective-area epitaxy (SAE) on a templated substrate [3], [4]. Numerous VNW-MOSFET demonstrations have been published with NWs grown using either of these techniques [56]–[58].

Reactive Ion Etching, in combination with digital etch, has recently emerged as a technique capable of creating very high aspect ratio nanowires in the InGaAs system that feature smooth vertical walls and dimensions in the nanometer range [59], [60]. A particularly spectacular example is shown in Fig. 10. Digital etch allows the controlled trimming of nanowire diameter while preserving the aspect ratio of the structure and improving sidewall smoothness. InGaAs VNW-MOSFETs have been demonstrated by this technique with performance that matches that of transistors fabricated by bottom-up approaches [61]. The use of digital etch was shown to improve both the subthreshold characteristics as well as  $g_m$  presumably as a result of removing a thin damaged subsurface layer at the sidewalls.

While the ON-state characteristics are still below what is desirable (mostly due to difficulties with the top contact), OFF-state behavior of InGaAs VNW-MOSFETs is approaching ideal behavior. Fig. 11 shows the linear subthreshold swing of InGaAs VNW MOSFETs vs. the ratio of the gate length to the electrostatic characteristic length,  $\lambda_c$ . For reference, the ideal behavior is also indicated [62]. A number

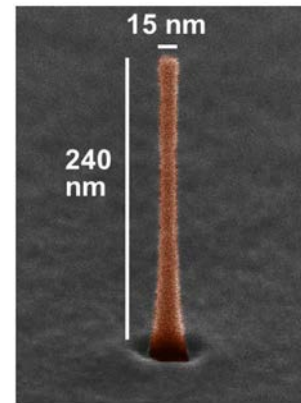


**FIGURE 10.** InGaAs nanowire fabricated by a combination of BCl/SiCl/Ar Reactive Ion Etching and digital etch [59].

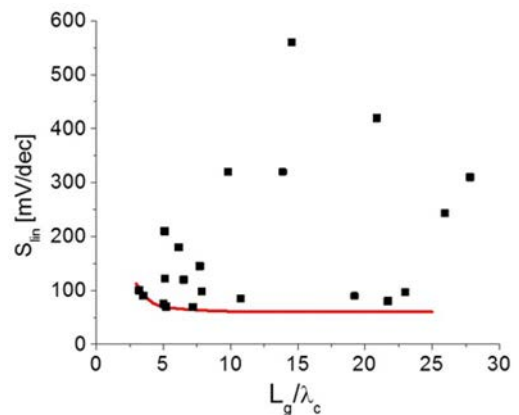


**FIGURE 11.** Linear subthreshold swing vs. ratio of gate length to electrostatic characteristic length of InGaAs VNW MOSFETs. For reference, the ideal electrostatic behavior is also indicated [62].

of device demonstrations already approach the theoretical expectations for this device architecture.

A challenge for InGaAs VNW-MOSFETs is scaling the nanowire diameter to the sub-10 nm regime. To date, the most aggressive VNW MOSFETs that have been demonstrated feature a 28 nm diameter [57], [58]. At a hypothetical point of insertion in the roadmap, nanowire diameters in the 7 nm range are needed [47]. At this scale, top contact resistance is a very significant problem. Additionally, nanowire survival during the fabrication process is a great concern.

#### V. INGAAS P-TYPE MOSFETS

We now turn our attention to p-channel MOSFETs. Among all III-V semiconductors, the antimonide system, specifically  $\text{In}_x\text{Ga}_{1-x}\text{Sb}$  with  $0 < x < 1$ , has recently attracted considerable attention due to its high hole mobility and its strong enhancement through compressive stress [1], [63], [64]. Significant progress has been made in the last few years towards InGaSb p-channel MOSFETs [64]–[67]. Remarkable improvements in the transport characteristics have been reported when biaxial [68]–[70] or uniaxial compressive strain [6] is applied.

Until recently, one of the challenges hampering the development of high-performance antimonide-based p-channel MOSFETs has been the lack of low-resistance ohmic contact technology. Recently, a new  $p^+$ -InAs/InAsSb composite cap structure has resulted in Au-based contacts to antimonide heterostructures with contact resistivities approaching  $1 \Omega \cdot \mu\text{m}^2$  [71]. In a more recent development, Au-less ohmic contacts have been achieved with contact resistivities just slightly higher [7]. These achievements bode well for the future of this device technology. Theoretical calculations of the Landauer limit for ohmic contact resistivity for this material system also suggest that significant improvements are to be expected [35].

A second critical requirement of an antimonide-based MOSFET is a high quality high-K oxide/semiconductor interface. Because of the highly reactive nature of antimonide compounds, surface passivation of GaSb or InGaSb is challenging. In recent years, several cleaning and passivation techniques have been proposed [72]–[75]. Among those, an HCl clean has been found to be an effective way to remove native oxides of GaSb. A lowest  $D_{it}$  value of  $3 \times 10^{11} \text{ eV}^{-1} \cdot \text{cm}^{-2}$  [76] and a minimum subthreshold swing of 120 mV/dec [66] have been reported. Excellent planar MOSFETs [67] have been demonstrated that suggest significant performance potential for this material system.

As with InGaAs, in order to deploy InGaSb as a channel material in a future generation of CMOS technology, a multigate 3D structure is necessary. Recently, the first InGaSb p-channel FinFETs have been demonstrated [7]. Achieving this milestone required the development of dry-etch technology capable of creating high-aspect ratio fins with vertical sidewalls. As Fig. 12 shows, a novel  $\text{BCl}_3/\text{N}_2$  RIE chemistry has made possible sub-20 nm wide InGaSb fins with vertical sidewalls and aspect ratio greater than 10. Also, dense fin patterns with excellent fin characteristics have been realized.

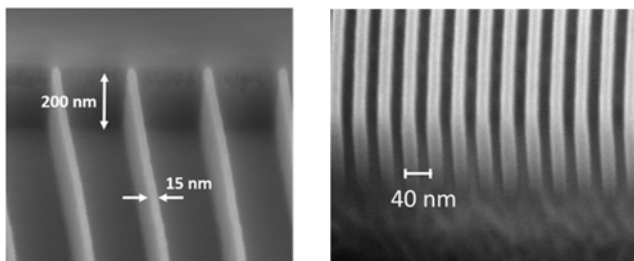


**FIGURE 12.** SEM images of sub-20 nm InGaSb (a) fins and (b) dense fin array with 20 nm fin spacing [7].

An encouraging finding about this RIE technology is the excellent electrical quality of the dry etched sidewalls after a light HCl etch treatment [7]. At least, this is the case for GaSb where initial experiments suggest a relatively low interface state density on the sidewall MOS structure. For InGaSb, the HCl chemical treatment is not suitable as it is

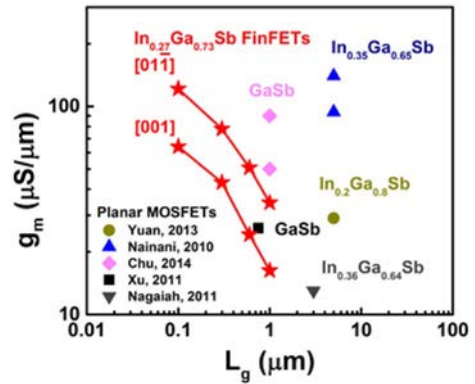


**FIGURE 13.** Maximum  $g_m$  vs.  $L_g$  of recently published InGaSb MOSFETs. All devices but the ones indicated by red stars are planar MOSFETs. The red star devices are FinFETs [7]. The strong orientation dependence of these devices suggests the important role of compressive uniaxial strain in hole transport.

difficult to control. A digital-etch process, similar to that used in the InGaAs system [60], is required for InGaSb-based heterostructures.

The first InGaSb FinFETs feature fin widths as narrow as 30 nm and gate lengths down to 100 nm [7]. These are double-gate devices with carrier modulation taking place only through the sidewalls. In spite of this, these devices show promising electrical characteristics with a  $g_m$  (normalized by gate periphery) that approaches that of the best InGaSb planar MOSFETs. This highlights the excellent quality of the sidewalls that this process is capable of. A summary of the state of the art is shown in Fig. 13. The first InGaSb FinFETs also manifest a prominent orientation dependence. This suggests that the process of fin formation partially relaxes the as-grown biaxially strained channel resulting in a strong uniaxial compressive strain in the direction of hole transport [7].

The ultimate potential of the antimonide material system for logic p-type MOSFETs is uncertain as limited research has been carried out to date. Fast progress has recently been made in contacts, high-quality MOS stacks and high aspect ratio etching. This suggests substantial promise. However, the technology remains relatively immature when compared with alternatives (most prominently, Ge p-MOSFETs).

## VI. CONCLUSION

Impressive recent III-V MOSFET progress gives hope for Moore's law to continue beyond the point where Si can reach. Planar and multigate InGaAs MOSFETs exhibit nearly ideal electrostatic scaling behavior. This bodes well for the potential of further scaling. However, device performance is still lacking particularly in scaled multigate designs. To overcome this problem, new research in low parasitic contact schemes and self-aligned designs is required. Recent progress in p-type InGaSb MOSFETs shows the promise of this material system for future nanoscale CMOS.

## ACKNOWLEDGMENT

III-V transistor and test structure fabrication at MIT is carried out in the fab facilities of the Microsystems Technology Laboratories and the Electron Beam Lithography Facility.

## REFERENCES

- [1] J. A. del Alamo, "Nanometre-scale electronics with III-V compound semiconductors," *Nature*, vol. 479, pp. 317–323, Nov. 2011.
- [2] J. A. del Alamo, "The high-electron mobility transistor at 30: Impressive accomplishments and exciting prospects," in *Proc. Int. Conf. Compd. Semicond. Manuf. Technol. (CS MANTECH)*, Palm Springs, CA, USA, May 2011, pp. 17–22.
- [3] H. Riel, L.-E. Wernersson, M. Hong, and J. A. del Alamo, "III-V compound semiconductor transistors—From planar to nanowire structures," *MRS Bull.*, vol. 39, pp. 668–677, Aug. 2014.
- [4] C. Zhang and X. Li, "III-V nanowire transistors for low-power logic applications: A review and outlook," *IEEE Trans. Electron Devices*, vol. 63, no. 1, pp. 223–234, Jan. 2016.
- [5] J. A. del Alamo *et al.*, "InGaAs MOSFETs for CMOS: Recent advances in process technology," in *Proc. IEEE Int. Electron Devices Meeting*, Washington, DC, USA, Dec. 2013, pp. 24–27.
- [6] L. W. Guo *et al.*, "Enhancing p-channel InGaSb QW-FETs via process-induced compressive uniaxial strain," *IEEE Electron Device Lett.*, vol. 35, no. 11, pp. 1088–1090, Nov. 2014.
- [7] W. Lu, J. K. Kim, J. F. Klem, S. D. Hawkins, and J. A. del Alamo, "An InGaSb p-channel FinFET," in *Proc. IEEE Int. Electron Devices Meeting*, Washington, DC, USA, Dec. 2015, pp. 819–822.
- [8] J. Lin, X. Cai, Y. Wu, D. A. Antoniadis, and J. A. del Alamo, "Record maximum transconductance of 3.45 mS/um for III-V FETs," *IEEE Electron Device Lett.*, vol. 37, no. 4, pp. 381–384, Apr. 2016.
- [9] W. E. Spicer, I. Lindau, P. Skeath, and C. Y. Su, "Unified defect model and beyond," *J. Vac. Sci. Technol.*, vol. 17, no. 5, pp. 1019–1027, 1980.
- [10] P. D. Ye *et al.*, "GaAs metal-oxide-semiconductor field-effect transistor with nanometer-thin dielectric grown by atomic layer deposition," *Appl. Phys. Lett.*, vol. 83, no. 1, pp. 180–182, Jul. 2003.
- [11] Y. Xuan, H. C. Lin, P. D. Ye, and G. D. Wilk, "Capacitance-voltage studies on enhancement-mode InGaAs metal-oxide-semiconductor field-effect transistor using atomic-layer-deposited Al<sub>2</sub>O<sub>3</sub> gate dielectric," *Appl. Phys. Lett.*, vol. 88, Jul. 2006, Art. no. 263518.
- [12] R. Engel-Herbert, Y. Hwang, and S. Stemmer, "Comparison of methods to quantify interface trap densities at dielectric/III-V semiconductor interfaces," *J. Appl. Phys.*, vol. 108, Dec. 2010, Art. no. 124101.
- [13] S. Oktyabrsky and P. D. Ye, Eds., *Fundamentals of III-V Semiconductor MOSFETs*. New York, NY, USA: Springer, 2010.
- [14] G. Brammert *et al.*, "A combined interface and border trap model for high-mobility substrate metal-oxide-semiconductor devices applied to In<sub>0.53</sub>Ga<sub>0.47</sub>As and InP capacitors," *IEEE Trans. Electron Devices*, vol. 58, no. 11, pp. 3890–3897, Nov. 2011.
- [15] M. Radosavljevic *et al.*, "Electrostatics improvement in 3-D tri-gate over ultra-thin body planar InGaAs quantum well field effect transistors with high-K gate dielectric and scaled gate-to-drain/gate-to-source separation," in *IEDM Tech. Dig.*, Washington, DC, USA, 2011, pp. 33.1.1–33.1.4.
- [16] J. Lin, D. A. Antoniadis, and J. A. del Alamo, "Sub-30 nm InAs quantum-well MOSFETs with self-aligned metal contacts and sub-1 nm EOT HfO<sub>2</sub> insulator," in *IEDM Tech. Dig.*, San Francisco, CA, USA, 2012, pp. 32.1.1–32.1.4.
- [17] S. Lee *et al.*, "Record ion (0.50 mA/um at VDD=0.5 V and Ioff=100 nA/um) 25 nm-gate-length ZrO<sub>2</sub>/InAs/InAlAs MOSFETs," in *Proc. Symp. VLSI Technol.*, Honolulu, HI, USA, 2014.
- [18] Y.-C. Lin *et al.*, "Low interface trap density Al<sub>2</sub>O<sub>3</sub>/In<sub>0.53</sub>Ga<sub>0.47</sub>As MOS capacitor fabricated on MOCVD-grown InGaAs epitaxial layer on Si substrate," *Appl. Phys. Exp.*, vol. 7, no. 4, 2014, Art. no. 041202.
- [19] N. Waldron *et al.*, "Gate-all-around InGaAs nanowire FETs with peak transconductance of 2200 uS/um at 50 nm Lg using a replacement fin RMG flow," in *Proc. IEEE Int. Electron Devices Meeting*, Washington, DC, USA, 2015, pp. 799–802.
- [20] J. Lin, D. A. Antoniadis, and J. A. del Alamo, "Novel intrinsic and extrinsic engineering for high-performance high-density self-aligned InGaAs MOSFETs: Precise channel thickness control and sub-40-nm metal contacts," in *Proc. IEEE Int. Electron Devices Meeting*, San Francisco, CA, USA, Dec. 2014, pp. 574–577.
- [21] J. Lin, D. A. Antoniadis, and J. A. del Alamo, "Impact of intrinsic channel scaling on InGaAs quantum-well MOSFETs," *IEEE Trans. Electron Devices*, vol. 62, no. 11, pp. 3470–3476, Nov. 2015.
- [22] J. Lin, D. A. Antoniadis, and J. A. del Alamo, "A CMOS-compatible fabrication process for scaled self-aligned InGaAs MOSFETs," in *Proc. 30th Int. Conf. Compd. Semicond. Manuf. Technol. (CS MANTECH)*, Scottsdale, AZ, USA, May 2015, p. 12.2.
- [23] M. Egard *et al.*, "High transconductance self-aligned gate last surface channel In<sub>0.53</sub>Ga<sub>0.47</sub>As MOSFET," in *IEDM Tech. Dig.*, Washington, DC, USA, 2011, pp. 303–306.
- [24] X. Zhou, Q. Li, C. W. Tang, and K. M. Lau, "30-nm inverted MOSHEMTs on Si substrate grown by MOCVD with regrown source/drain," *IEEE Electron Device Lett.*, vol. 33, no. 10, pp. 1384–1386, Oct. 2012.
- [25] S. Lee *et al.*, "Highly scalable raised source/drain InAs quantum well MOSFETs exhibiting I<sub>ON</sub> = 482 uA/um at I<sub>OFF</sub> = 100 nA/um and V<sub>DD</sub> = 0.5 V," *IEEE Electron Device Lett.*, vol. 35, no. 6, pp. 621–623, Jun. 2014.
- [26] S. W. Chang *et al.*, "InAs N-MOSFETs with record performance of I<sub>on</sub> = 600 uA/um at I<sub>off</sub> = 100 nA/um (V<sub>d</sub> = 0.5 V)," in *Proc. Int. Electron Devices Meeting*, Washington, DC, USA, 2013, pp. 417–420.
- [27] R. Oxland *et al.*, "An ultralow-resistance ultrashallow metallic source/drain contact scheme for III-V NMOS," *IEEE Electron Device Lett.*, vol. 33, no. 4, pp. 501–503, Apr. 2012.
- [28] S. Kim *et al.*, "Self-aligned metal source/drain In<sub>x</sub>Ga<sub>1-x</sub>As n-metal-oxide-semiconductor field-effect transistors using Ni-InGaAs alloy," *Appl. Phys. Exp.*, vol. 4, no. 2, Jan. 2011, Art. no. 024201.
- [29] X. Zhang *et al.*, "In<sub>0.7</sub>Ga<sub>0.3</sub>As channel n-MOSFET with self-aligned Ni-InGaAs source and drain," *Electrochem. Solid-State Lett.*, vol. 14, no. 2, pp. H60–H62, 2011.
- [30] Y. Sun *et al.*, "High-performance CMOS-compatible self-aligned In<sub>0.53</sub>Ga<sub>0.47</sub>As MOSFETs with G<sub>MSAT</sub> over 2200 μS/μm at V<sub>DD</sub> = 0.5 V," in *Proc. IEDM*, San Francisco, CA, USA, 2014, pp. 582–585.
- [31] J. Lin, D. A. Antoniadis, and J. A. del Alamo, "InGaAs quantum-well MOSFET arrays for nanometer-scale ohmic contact characterization," *IEEE Trans. Electron Devices*, vol. 63, no. 3, pp. 1020–1026, Mar. 2016.
- [32] R. Dormaier and S. E. Mohny, "Factors controlling the resistance of ohmic contacts to n-InGaAs," *J. Vac. Sci. Technol. B*, vol. 30, no. 3, May 2012, Art. no. 031209.
- [33] W. Lu, A. Guo, A. Vardi, and J. A. del Alamo, "A test structure to characterize nano-scale ohmic contacts in III-V MOSFETs," *IEEE Electron Device Lett.*, vol. 35, no. 2, pp. 178–180, Feb. 2014.
- [34] T.-W. Kim, D.-H. Kim, and J. A. del Alamo, "60 nm self-aligned-gate InGaAs HEMTs with record high-frequency characteristics," in *Proc. IEEE Int. Electron Devices Meeting*, San Francisco, CA, USA, 2010, pp. 696–699.
- [35] A. Baraskar, A. C. Gossard, and M. J. W. Rodwell, "Lower limits to metal-semiconductor contact resistance: Theoretical models and experimental data," *J. Appl. Phys.*, vol. 114, Oct. 2013, Art. no. 154516.
- [36] J. Lin, D. A. Antoniadis, and J. A. del Alamo, "Off-state leakage induced by band-to-band tunneling and floating-body bipolar effect in InGaAs quantum-well MOSFETs," *IEEE Electron Device Lett.*, vol. 35, no. 12, pp. 1203–1205, Dec. 2014.
- [37] J. Lin, D. A. Antoniadis, and J. A. del Alamo, "Physics and mitigation of excess OFF-state current in InGaAs quantum-well MOSFETs," *IEEE Trans. Electron Devices*, vol. 62, no. 5, pp. 1448–1455, May 2015.
- [38] C. H. Jan *et al.*, "A 22nm SoC platform technology featuring 3-D tri-gate and high-k/metal gate, optimized for ultra low power, high performance and high density SoC applications," in *Proc. IEDM*, San Francisco, CA, USA, 2012, pp. 44–47.
- [39] S. Natarajan *et al.*, "A 14nm logic technology featuring 2nd-generation FinFET, air-gapped interconnects, self-aligned double patterning and a 0.0588 m<sup>2</sup> SRAM cell size," in *Proc. IEDM*, San Francisco, CA, USA, 2014, pp. 71–73.
- [40] H.-C. Chin *et al.*, "III-V multiple-gate field-effect transistors with high-mobility In<sub>0.7</sub>Ga<sub>0.3</sub>As channel and epi-controlled retrograde-doped fin," *IEEE Electron Device Lett.*, vol. 32, no. 2, pp. 146–148, Feb. 2011.



- [41] T.-W. Kim *et al.*, "Sub-100 nm InGaAs quantum-well (QW) tri-gate MOSFETs with Al<sub>2</sub>O<sub>3</sub>/HfO<sub>2</sub> (EOT<1 nm) for low-power applications," in *Proc. IEEE Int. Electron Devices Meeting*, Washington, DC, USA, Dec. 2013, pp. 425–428.
- [42] N. Waldron *et al.*, "An InGaAs/InP quantum well FinFET using the replacement fin process integrated in an RMG flow on 300mm Si substrates," in *IEEE Symp. VLSI Technol. Tech. Dig.*, Honolulu, HI, USA, 2014, pp. 1–2.
- [43] A. V. Thathachary *et al.*, "Indium arsenide (InAs) single and dual quantum-well heterostructure FinFETs," in *Proc. IEEE Symp. VLSI Technol.*, Kyoto, Japan, 2015, pp. T208–T209.
- [44] R. Oxland *et al.*, "InAs FinFETs with H<sub>fin</sub>=20 nm fabricated using a top-down etch process," *IEEE Electron Device Lett.*, vol. 37, no. 3, pp. 261–264, Mar. 2016.
- [45] A. Vardi, J. Lin, W. Lu, X. Zhao, and J. A. del Alamo, "High aspect ratio InGaAs FinFETs with sub-20 nm fin width," in *Proc. Symp. VLSI Technol.*, 2016, to be published.
- [46] J. G. Fiorenza *et al.*, "Aspect ratio trapping: A unique technology for integrating Ge and III-Vs with silicon CMOS," *ECS Trans.*, vol. 33, no. 6, pp. 963–976, 2010.
- [47] D. Yakimets *et al.*, "Vertical GAAFETs for the ultimate CMOS scaling," *IEEE Trans. Electron Devices*, vol. 62, no. 5, pp. 1433–1439, May 2015.
- [48] A. Vardi, X. Zhao, and J. A. del Alamo, "InGaAs double-gate fin-sidewall MOSFETs," in *Proc. 72nd IEEE Device Res. Conf.*, Santa Barbara, CA, USA, Jun. 2014, pp. 219–220.
- [49] T. Ivanov *et al.*, "The influence of post-etch InGaAs fin profile on electrical performance," *Jpn. J. Appl. Phys.*, vol. 53, no. 4S, 2014, Art. no. 04EC20.
- [50] A. Vardi, W. Lu, X. Zhao, and J. A. del Alamo, "Nanoscale Mo ohmic contacts to III-V fins," *IEEE Electron Device Lett.*, vol. 36, no. 2, pp. 126–128, Feb. 2015.
- [51] C.-W. Lee, S.-R.-N. Yun, C.-G. Yu, J.-T. Park, and J.-P. Colinge, "Device design guidelines for nano-scale MuGFETs," *Solid State Electron.*, vol. 51, no. 3, pp. 505–510, 2007.
- [52] N. Agrawal, Y. Kimura, R. Arghavani, and S. Datta, "Impact of transistor architecture (bulk planar, trigate on bulk, ultrathin-body planar SOI) and material (silicon or III-V semiconductor) on variation for logic and SRAM applications," *IEEE Trans. Electron Devices*, vol. 60, no. 10, pp. 3298–3304, Oct. 2013.
- [53] A. Vardi, X. Zhao, and J. A. del Alamo, "Quantum-size effects in sub 10 nm fin width InGaAs FinFETs," in *Proc. IEEE Int. Electron Devices Meeting*, Washington, DC, USA, Dec. 2015, pp. 807–810.
- [54] J. J. Gu *et al.*, "First experimental demonstration of gate-all-around III-V MOSFETs by top-down approach," in *IEDM Tech. Dig.*, Washington, DC, USA, 2011, pp. 33.2.1–33.2.4.
- [55] A. V.-Y. Thean *et al.*, "Vertical device architecture for 5nm and beyond: Device & circuit implications," in *Proc. VLSI Technol. Symp.*, 2015, pp. T26–T27.
- [56] K. Tomioka, M. Yoshimura, and T. Fukui, "A III-V nanowire channel on silicon for high-performance vertical transistors," *Nature*, vol. 488, no. 7410, pp. 189–192, 2012.
- [57] K.-M. Persson *et al.*, "Extrinsic and intrinsic performance of vertical InAs nanowire MOSFETs on Si substrates," *IEEE Trans. Electron Devices*, vol. 60, no. 9, pp. 2761–2767, Sep. 2013.
- [58] M. Berg *et al.*, "Self-aligned, gate-last process for vertical InAs nanowire on Si," in *IEDM Tech. Dig.*, Washington, DC, USA, 2015, pp. 803–806.
- [59] X. Zhao and J. A. del Alamo, "Nanometer-scale vertical-sidewall reactive ion etching of InGaAs for 3-D III-V MOSFETs," *IEEE Electron Device Lett.*, vol. 35, no. 5, pp. 521–523, May 2014.
- [60] J. Lin, X. Zhao, D. A. Antoniadis, and J. A. del Alamo, "A novel digital etch technique for deeply scaled III-V MOSFETs," *IEEE Electron Device Lett.*, vol. 35, no. 4, pp. 440–442, Apr. 2014.
- [61] X. Zhao, J. Lin, C. Heidelberger, E. A. Fitzgerald, and J. del Alamo, "Vertical nanowire InGaAs MOSFETs fabricated by a top-down approach," in *Proc. Int. Electron Devices Meeting (IEDM)*, Washington, DC, USA, Dec. 2013, pp. 28.4.1–28.4.4.
- [62] C. P. Auth and J. D. Plummer, "Scaling theory for cylindrical, fully-depleted, surrounding-gate MOSFETs," *IEEE Electron Device Lett.*, vol. 18, no. 2, pp. 74–76, Feb. 1997.
- [63] L. Xia, B. Boos, B. R. Bennett, M. G. Ancona, and J. A. del Alamo, "Hole mobility enhancement through <110> uniaxial strain in In<sub>0.41</sub>Ga<sub>0.59</sub>Sb quantum-well field-effect transistors," *Appl. Phys. Lett.*, vol. 98, no. 5, 2011, Art. no. 053505.
- [64] M. Barth *et al.*, "Compressively strained InSb MOSFETs with high hole mobility for p-channel application," in *Proc. DRC*, Notre Dame, IN, USA, Jun. 2013, pp. 21–22.
- [65] M. Xu, R. Wang, and P. D. Ye, "GaSb inversion-mode PMOSFETs with atomic-layer-deposited Al<sub>2</sub>O<sub>3</sub> as gate dielectric," *IEEE Electron Device Lett.*, vol. 32, no. 7, pp. 883–885, Jul. 2011.
- [66] A. Nainani *et al.*, "Development of high-k dielectric for antimonides and a sub 350 °C III-V pMOSFET outperforming germanium," in *Proc. IEEE IEDM*, San Francisco, CA, USA, Dec. 2010, pp. 6.4.1–6.4.4.
- [67] A. Nainani *et al.*, "Optimization of the Al<sub>2</sub>O<sub>3</sub>/GaSb interface and a high-mobility GaSb pMOSFET," *IEEE Trans. Electron Devices*, vol. 58, no. 10, pp. 3407–3415, Oct. 2011.
- [68] B. R. Bennett *et al.*, "Mobility enhancement in strained p-InGaSb quantum wells," *Appl. Phys. Lett.*, vol. 91, no. 4, Jul. 2007, Art. no. 042104.
- [69] J. B. Boos *et al.*, "High mobility p-channel HFETs using strained Sb-based materials," *Electron. Lett.*, vol. 43, no. 15, pp. 834–835, Jul. 2007.
- [70] M. Radosavljevic *et al.*, "High-performance 40 nm gate length InSb p-channel compressively strained quantum well field effect transistors for low-power (V<sub>CC</sub> = 0.5 V) logic applications," in *Proc. IEEE IEDM*, San Francisco, CA, USA, Dec. 2008, pp. 1–4.
- [71] L. W. Guo, W. Lu, B. R. Bennett, J. B. Boos, and J. A. del Alamo, "Ultra-low resistance ohmic contacts for p-channel InGaSb field-effect transistors," *IEEE Electron Device Lett.*, vol. 36, no. 6, pp. 546–548, Jun. 2015.
- [72] M. Yokoyama, H. Yokoyama, M. Takenaka, and S. Takagi, "Impact of interfacial InAs layers on Al<sub>2</sub>O<sub>3</sub>/GaSb metal-oxide-semiconductor interface properties," *Appl. Phys. Lett.*, vol. 106, no. 12, 2015, Art. no. 122902.
- [73] K. Nishi *et al.*, "High hole mobility front-gate InAs/InGaSb-OI single structure CMOS on Si," in *Proc. Symp. VLSI Technol.*, Kyoto, Japan, 2015, pp. T174–T175.
- [74] L. Zhao, Z. Tan, J. Wang, and J. Xu, "Effects of ozone post deposition treatment on interfacial and electrical characteristics of atomic-layer-deposited Al<sub>2</sub>O<sub>3</sub> and HfO<sub>2</sub> films on GaSb substrates," *Appl. Surf. Sci.*, vol. 289, pp. 601–605, Jan. 2014.
- [75] R. L. Chu *et al.*, "Passivation of GaSb using molecular beam epitaxy Y<sub>2</sub>O<sub>3</sub> to achieve low interfacial trap density and high-performance self-aligned inversion-channel P-metal-oxide-semiconductor field-effect-transistors," *Appl. Phys. Lett.*, vol. 105, no. 18, 2014, Art. no. 182106.
- [76] A. Nainani *et al.*, "Device quality Sb-based compound semiconductor surface: A comparative study of chemical cleaning," *J. Appl. Phys.*, vol. 109, no. 11, 2011, Art. no. 114908.



**JESÚS A. DEL ALAMO** (S'79–M'85–SM'92–F'06) received the Telecommunications Engineer degree from the Polytechnic University of Madrid, in 1980, and the M.S. and Ph.D. degrees in electrical engineering from Stanford University, in 1983 and 1985, respectively. He has been with the Massachusetts Institute of Technology, since 1988, where he is currently the Donner Professor of Electrical Engineering, and the Director of the Microsystems Technology Laboratories.



**DIMITRI A. ANTONIADIS** (M'79–SM'83–F'90–LF'14) received the B.S. degree in physics from the National University of Athens, Greece, in 1970, and the M.S. and Ph.D. degrees in electrical engineering from Stanford University, in 1972 and 1976, respectively. He joined the Massachusetts Institute of Technology, in 1978, where he is currently the Ray and Maria Stata Professor of Electrical Engineering.



**JIANQIANG LIN** (S'08) received the B.Eng. (Hons.) and M.Eng. degrees in electrical engineering from the National University of Singapore, in 2007 and 2009, respectively, and the Ph.D. degree from the Massachusetts Institute of Technology, in 2015. He is currently the Enrico Fermi Post-Doctoral Fellow with Argonne National Laboratory.



**ALON VARDI** received the B.Tech. degree (*summa cum laude*) in electrical engineering from the University of Ariel, Ariel, Israel, in 2002, and the M.S. (*cum laude*) and Ph.D. degrees from the Department of Electrical Engineering, Technion—Israel Institute of Technology, Haifa, Israel, in 2006 and 2010, respectively. He joined the TowerJazz Research and Development Department, as a Senior Device Engineer. In 2012, he joined the Microsystems Technology Laboratories, MIT. His current research interest is III-V 3D electronic devices and diamond-based electronics.



**WENJIE LU** received the B.S. degrees in electrical engineering and mathematics from the University of Wisconsin—Madison, USA, in 2008. He is currently pursuing the Ph.D. degree with the Department of Electrical Engineering and Computer Science, Massachusetts Institute of Technology, Cambridge, MA, USA.

His current research interests include fabrication and transport physics of III-V MOSFETs, and the modeling of nano-scale low-resistance ohmic contacts.



**XIN ZHAO** received the B.S. degree in physics from Peking University, Beijing, China, in 2010, and the S.M. degree in materials science and engineering from the Massachusetts Institute of Technology, in 2012, where he is currently pursuing the Ph.D. degree

His current research interest is on III-V vertical nanowire transistor technologies for ultralow power applications.